

## EFFECT OF SCANNING METHODS IN THE SELECTIVE LASER MELTING OF 316L/TiC NANOCOMPOSITIES

B. AlMangour<sup>×\*</sup>, D. Grzesiak<sup>†</sup>, J. M. Yang<sup>×</sup>

<sup>×</sup>Department of Materials Science and Engineering, University of California Los Angeles, Los Angeles, CA 90095, USA

<sup>†</sup>Department of Mechanical Engineering and Mechatronics, West Pomeranian University of Technology, Szczecin, Poland

\*Corresponding author:

Email: balmangour@gmail.com

### Abstract

Selective laser melting (SLM) is a promising additive manufacturing process that allows for the fabrication of complex functional components by the selective layer-by-layer melting of particles on a powder bed using a high-energy laser beam. In this study, the SLM process was used to fabricate components of TiC/ 316L stainless steel nanocomposite using various laser scanning methods. The results showed that the laser-scanning method used for the SLM process affects the degree of densification, microstructure, and the hardness of the components produced. We believe that the alternative fabrication route presented in this study should significantly increase the use of nanocomposites.

**Keywords:** Selective Laser Melting; Porosity; Microstructure; Hardness

### Introduction

316L stainless steel alloy is of great interest in the industry for their superior ductility and excellent corrosion resistance [1]. However, the applications of these alloys have been limited due to their poor strength and wear resistance both at room and high temperatures [2, 3]. To overcome this problem, 316L alloys may be strengthened by a uniform dispersion of very hard fine ceramic particles [4], which can be then used in wear resistant and thermally stable environment.

Additive manufacturing (AM) has emerged as a key enabling technology to shorten the product development cycle [6]. AM refers to a class of advanced technologies that can directly use three-dimensional computer aided design data to automatically fabricate multifunctional parts in a layer-by-layer manner [5]. Selective laser melting (SLM) is a new and highly promising AM technique for fabricating complex geometry parts by the selective melting of a metal powder and its subsequent rapid solidification [6]. The layer-wise addition process and the high thermal-energy gradients of the laser during SLM processing cause the crystals to grow preferentially (i.e., they cause directional solidification) [7]. Therefore, the scanning methods used during the SLM fabrication process can lead to significantly different degrees of densification as well as variations in the microstructure and texture and hence different mechanical properties (i.e., the SLM process can determine the anisotropy of the mechanical properties of the fabricated components).

In a previous work [8], we had studied the effects of the TiC volume content and particle size on the microstructure and mechanical properties of the resulting composite. In this work, a composite consisting of 316L stainless steel reinforced with 15% (vol.) TiC was produced by SLM using four different laser-scanning methods. The effects of the scanning method used on the solidification microstructure formed were investigated using scanning electron microscopy (SEM), and X-ray diffraction (XRD) analysis. The anisotropy in the mechanical properties of the produced material was analyzed based on the hardness.

### Experimental procedures

#### Feedstock powder, and SLM processes

The starting powder materials were: water-atomized 316L having an irregular shape and an average particle size of 45  $\mu\text{m}$  (Fig. 1a), and pure titanium carbide (TiC) with a mean particle size of 1  $\mu\text{m}$  (Fig. 1b). A powder mixture containing 85 vol.% 316L, 15 vol.% TiC was mechanically alloyed under a vacuum atmosphere using a Pulverisette 6 planetary high-energy ball mill. The milling conditions and parameters used for powder preparation are discussed in our previous work [8]. Cylindrical specimens with dimensions of 8 mm x 10 mm were produced according to the SLM processing parameters highlighted in Table 1 and with different scanning methods, shown in Fig. 2.

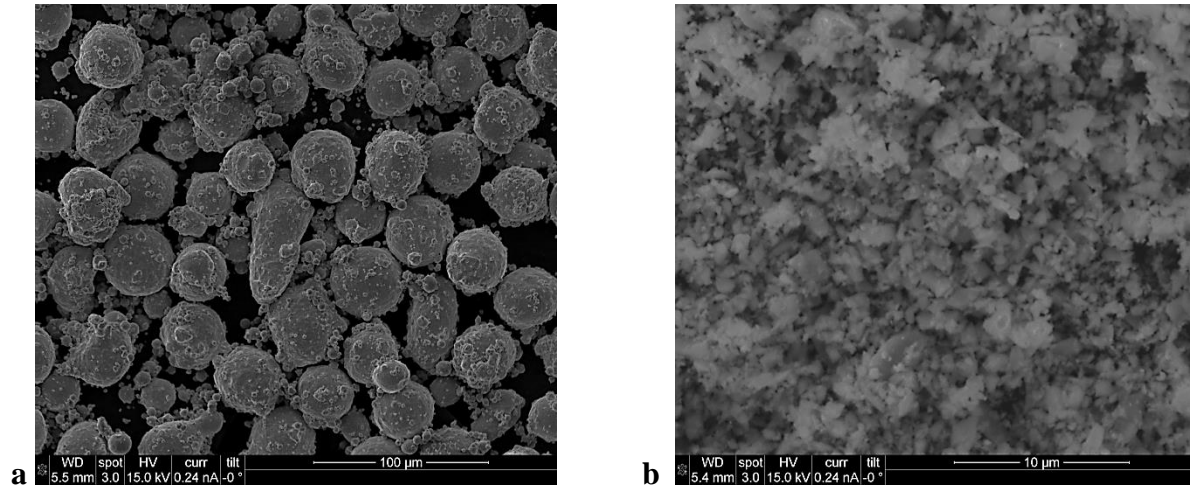


**Figure 1:** SEM micrograph of (a) 316L stainless steel powder; (b) TiC powder.

**Table 1:** SLM processing parameters

Laser power	Atmosphere	Scanning speed	Layer thickness
100 W	Argon	250 mm/sec	50 $\mu\text{m}$

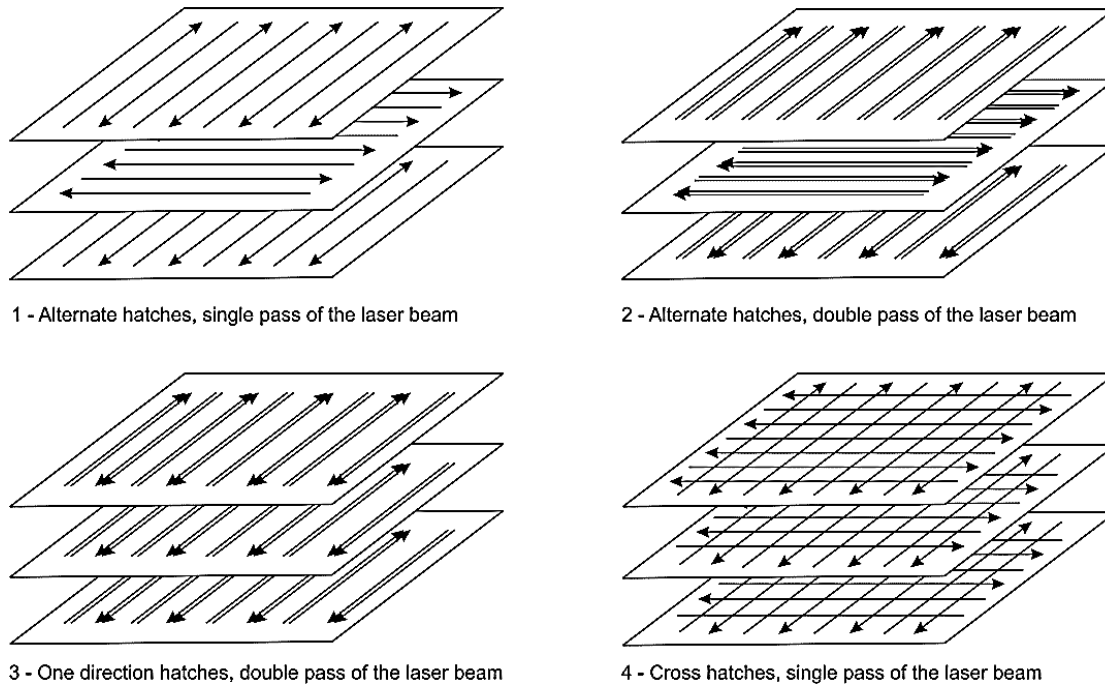


**Figure 2:** Scanning methods implemented in the current study.

### Microstructural and mechanical characterizations

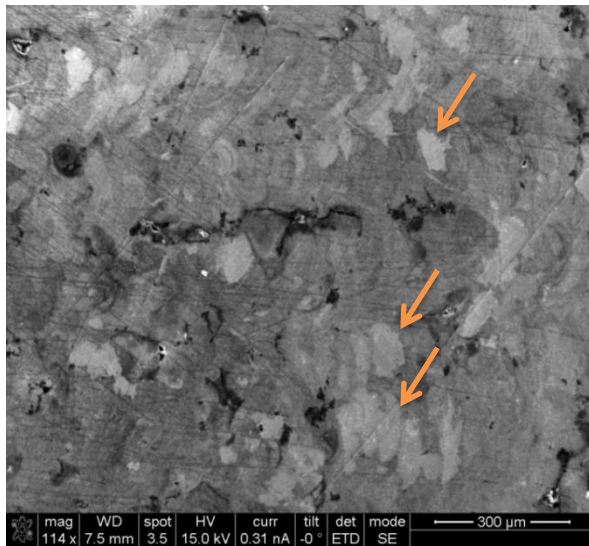
Samples were mechanically grounded and polished with progressively finer grit papers using the standard metallographic techniques and etched in Marble's Reagent for 10 s. The cross-sectional microstructures of the SLM-processed nanocomposites were observed using a Nova 230 Nano scanning electron microscope (SEM). XRD measurements were conducted on a PANalytical X'Pert PRO X-ray powder diffractometer (XRD) instrument, operating with a cobalt anticathode at 35 kV and 40 mA using a continuous scan mode at 5° /min. The relative densities were measured by the conventional “Archimedes' principle”.

Vickers indentations was performed (Leco, LM800AT) at a load of 200 g at 15 random locations.

## Results and Discussion

### Microstructural characterizations

Figure 3 shows low-magnification image of the side-view microstructure (i.e. along the building direction) of the SLM-processed nanocomposite using scanning-3 method after etching. The individual long-scan tracks (see the arrows in Fig. 3) and the cross-sections of the melt pools, represented by the half-cylinders/crescents, can be seen clearly. From Fig. 3, it can be seen that the width of the individual scan tracks/grain width was approximately equal to the hatch spacing (~120 μm.). The widths of the melt pools varied from 110±10 to 170±15 μm, based on the cross-sections of the melt pools; these values were higher than the layer thickness. Further, the melt pools were not always continuous, owing to variations in the depth and shape of the pools.



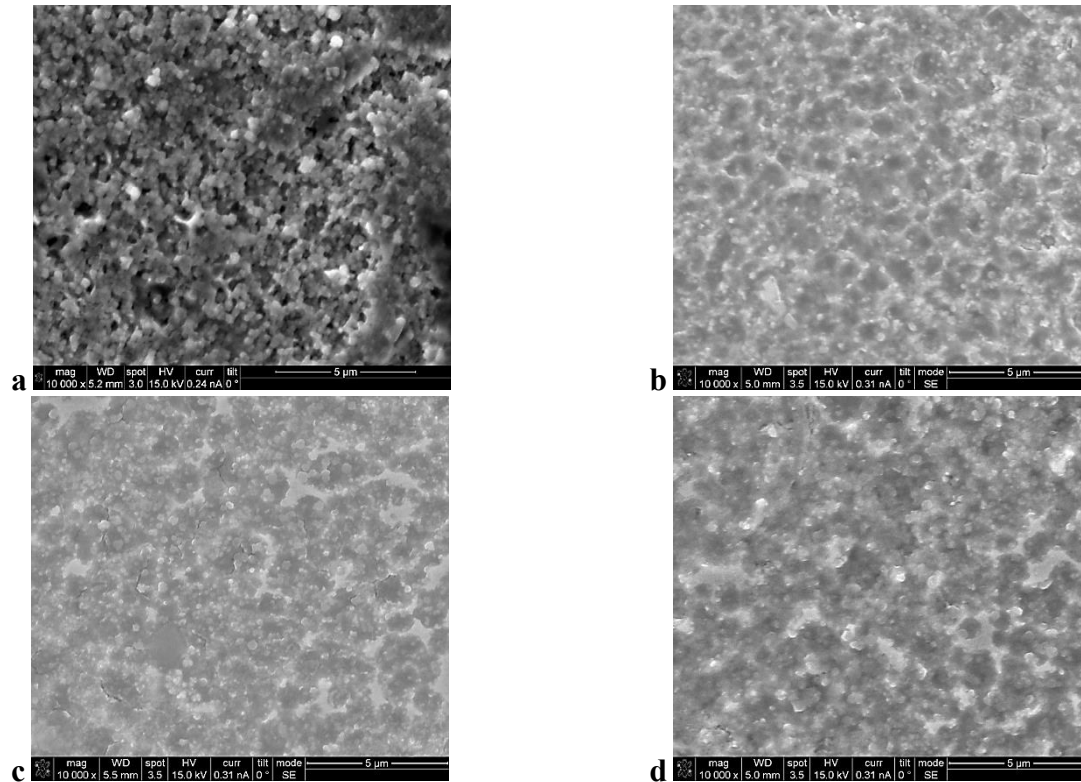
**Figure 3:** Cross-sectional microstructure of the SLM-processed TiC/316L nanocomposite processed using scanning-3 method.

Figure 4 shows high-magnification side-view (i.e. along the building direction) SEM images of the SLM-processed nanocomposites. In general, all composites sample shows very fine grain size as a result of fast cooling. The grains are of different sizes, may be due to the varying thermal heat fluxes during every scanning tracks. Apart, more importantly, one can observe the influence of the scanning method used on the resulting microstructure. The grain structures were clearly affected by the geometry of the melting pool, as heat flow and grain growth occurred perpendicular to the liquidus/solidus interface, leading to the morphology observed.

In general, the microstructure of SLM-fabricated components is characterized by discontinuous columnar grains/dendrites, whose orientation is determined by the heat-flow direction, which depends on the movement of the laser beam. It can be seen from Fig. 4 that the solidification morphology was highly correlated with the SLM building method. The dendrites had a distinct columnar structure aligned along the building direction, in a manner similar to the case in a directionally solidified microstructure. Further, on comparing Figs. 4a and 4b, it can be seen that the size of the dendrites was significantly affected by laser remelting during double scanning. Refinement in columnar structure is done by laser re-melting which is reported in earlier reports [9-11]. With double-pass scanning, the remelting of the solidified layer in the second pass of the laser beam causes the dendrites to become finer than those seen in Fig. 4a. Further, during the second pass, the laser beam is focused on the already-solidified material whereas it is focused on powder particles in the first scan. Thus, in the second pass, less energy is absorbed and heat is conducted away more quickly. As a result, the size of the melt pools in the second pass is smaller and some of the material created in the first scan still remains in the final product. A higher number of particle interfaces are broken down in the second pass, and a large number of pore defects are eliminated. The presence of pores retards recrystallization by pinning the dislocations and boundaries necessary for the process [12], and the reduction in porosity during the second pass enhances the recrystallization of the double-pass samples. The smaller

grain sizes of the double-pass nanocomposite components could be attributed to all of these factors.

The samples formed using unidirectional hatches with double scanning (scanning method 3) exhibited two solidification modes (solidification structure consisting of cellular dendrites mixed with equiaxed grains), while in the samples produced using the cross-hatches scanning method (scanning method 4), the solidification microstructure mainly consisted of fine equiaxed grains with a size smaller than 2  $\mu\text{m}$  (Fig. 4d). Further, it was evident that the TiC nanoparticles were present both within and at the grain boundaries.



**Figure 4:** Etched top-view microstructure of the SLM-processed nanocomposite: (a) scanning 1; (b) scanning 2; (c) scanning 3; (d) scanning 4.

Table 2 shows the effect of applied scanning methods on the densification level. It is evident that the building orientation had a pronounced effect on the density, which is typical for SLM processing. Remelting (by performing laser scanning twice) caused more uniform and smoother layers to appear and efficiently reduced the number of pores formed between the neighboring melt pools at the edges of the scan track. When the dual-pass scanning method was used, the voids between the adjacent laser tracks largely disappeared and higher-density parts with a smooth and defect-free surface were produced (Table 2). Previous studies have shown the potential effect of laser remelting on the densification level and surface roughness [10, 11]. It was seen that, with double scanning, the flowability of the melt as well as the rheological properties were enhanced. Hence, the molten 316L with the reinforcing TiC particles are sufficiently high, leading to more homogeneous and efficient mass and heat transfer in the pool.

**Table 2:** Theoretical relative density of the SLM-processed nanocomposite.

Scanning type	1	2	3	4
Relative density (%)	92.48	96.04	86.91	96.40

### XRD analysis

Figure 5 shows the typical XRD histogram for the SLM-processed nanocomposites using different scanning methods. The XRD pattern of the as-built samples exhibits a significant peak broadening due to the grain refinements as a result of fast cooling. Strong diffraction peaks related to austenitic stainless steel and corresponding to  $\gamma$ -Fe as well as diffraction peaks attributable to the TiC phase were seen in the case of all the samples. This confirmed the formation of TiC-reinforced 316L nanocomposites after SLM processing using different scanning methods. The high cooling rate during the SLM process caused the fabricated nanocomposites to contain an  $\alpha$ -Fe phase in a small fraction.

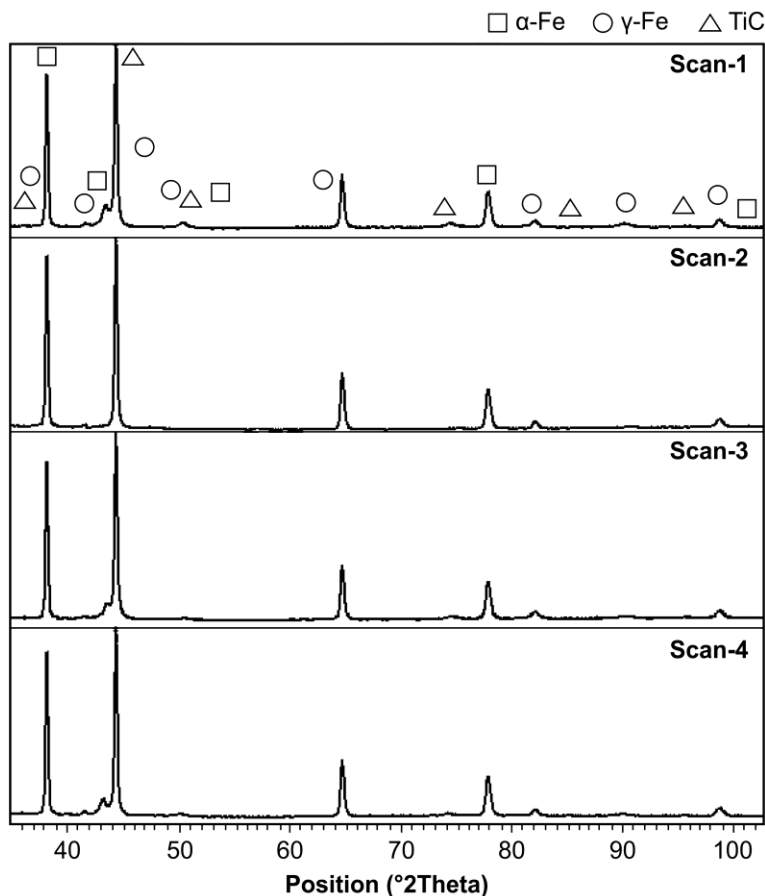


**Figure 5:** XRD histogram for the as-built nanocomposite using different scanning methods.

## Mechanical behavior

Table 3 demonstrates the effect of the applied SLM scanning method on microhardness. The observed increase in the hardness could primarily be attributed to grain boundary strengthening and grain refinement and to the presence of the ( $\alpha$ -Fe) phase. In general, the scanning methods seemed to have an effect on the hardness values. Indeed, the porosity level, grain refinement (Hall-Petch relation), and homogeneity of particle distribution (greater homogeneity resulted in greater dispersion strengthening) played significant roles in determining the mechanical properties of the SLM products. Further, it was evident that the double-pass scanning method resulted in higher hardness; this was because of the additional grain refinement of the fabricated nanocomposite and an improvement in the homogeneity of the particle distribution (i.e., to dispersion hardening being effective) as well as an increase in the density.

**Table 3:** Variation of microhardness as a function of the applied scanning method.

Scanning type	1	2	3	4
Microhardness (HV <sub>0.2</sub> )	383.87	430.92	370.86	365.3

## Conclusions

TiC/316L nanocomposites have been successfully produced by SLM process, and the effects of scanning methods on the microstructure and mechanical properties were studied. The findings of this study would be a valuable reference when selecting the proper scanning method for the SLM fabrication of 316L nanocomposite samples with the desirable grain structure and mechanical properties.

## Acknowledgment

One of the authors, Bandar AlMangour, would like to extend his appreciation to the Saudi Basic Industries Corporation, which generously awarded financial support to him.

## References

- [1] AL-Mangour B. Powder Metallurgy of Stainless Steel: State-of-the Art, Challenges, and Development. Stainless Steel: Microstructure, Mechanical Properties and Methods of Application: Nova Science Publishers; 2015. p. pp. 37-80.
- [2] Krishna DSR, Sun Y. Effect of thermal oxidation conditions on tribological behaviour of titanium films on 316L stainless steel. Surface and Coatings Technology 2005;198:447-53.
- [3] Majumdar JD, Kumar A, Li L. Direct laser cladding of SiC dispersed AISI 316L stainless steel. Tribology International 2009;42:750-3.
- [4] Abenojar J, Velasco F, Torralba J, Bas J, Calero J, Marce R. Reinforcing 316L stainless steel with intermetallic and carbide particles. Materials Science and Engineering: A 2002;335:1-5.
- [5] Gibson I, Rosen D, Stucker B. Additive manufacturing technologies: 3D printing, rapid prototyping, and direct digital manufacturing: Springer; 2014.
- [6] Yap C, Chua C, Dong Z, Zhang D, Loh L, et al. Review of selective laser melting: Materials and applications. Applied Physics Reviews 2015;2:041101.
- [7] Murr LE, Gaytan SM, Ramirez DA, Martinez E, Hernandez J, Amato KN, et al. Metal fabrication by additive manufacturing using laser and electron beam melting technologies. Journal of Materials Science & Technology 2012;28:1-14.

- [8] AlMangour B, Grzesiak D, Yang J-M. Selective laser melting of TiC reinforced 316L stainless steel matrix nanocomposites: Influence of starting TiC particle size and volume content. *Materials & Design* 2016.
- [9] Yasa E, Deckers J, Kruth J-P. The investigation of the influence of laser re-melting on density, surface quality and microstructure of selective laser melting parts. *Rapid Prototyping Journal* 2011;17:312-27.
- [10] Yasa E, Kruth J-P. Microstructural investigation of Selective Laser Melting 316L stainless steel parts exposed to laser re-melting. *Procedia Engineering* 2011;19:389-95.
- [11] Xie J, Fox P, O'Neill W, Sutcliffe C. Effect of direct laser re-melting processing parameters and scanning strategies on the densification of tool steels. *Journal of materials processing technology* 2005;170:516-23.
- [12] Rollett A, Humphreys F, Rohrer GS, Hatherly M. *Recrystallization and related annealing phenomena*: Elsevier; 2004.